2010 NDIA GROUND VEHICLE SYSTEMS ENGINEERING AND TECHNOLOGY SYMPOSIUM
MODELING & SIMULATION, TESTING AND VALIDATION (MSTV) MINI-SYMPOSIUM
AUGUST 17-19 DEARBORN, MICHIGAN

ANALYSIS AND DESIGN OF A NONLINEAR ACTIVE SUSPENSION SYSTEM INCORPORATING A NEGATIVE STIFFNESS SPRING

Robert N. K. Loh
Witt Thanom
Derrick Brock
Center for Robotics and Advanced Automation
School of Engineering and Computer Science
Oakland University, Rochester, MI

ABSTRACT

The analysis and design of a novel active suspension system incorporating a negative stiffness spring are investigated in this paper. The suspension structure consists of the mechanism that employs a combination of ordinary and negative stiffness springs and damping element. The resulting system yields superior performance in terms of mobility, maneuverability, and stability, particularly in harsh terrains and/or off-road environment. However, its dynamics are highly nonlinear and cannot be handled directly by conventional design techniques and methodologies. In this paper, the formulation of the proposed active suspension system consists of two phases: analysis and synthesis. In the analysis phase, nonlinear controls based on the advanced feedback linearization methodologies of the differential geometric theory is considered. The approach renders the difficult task of developing nonlinear controls rather simple. In the synthesis phase, which is required for real-world implementation and mechanization, observer-based controls are conducted. Extensive simulation studies show that the system can effectively reject all the harsh road disturbances while stabilizing the vehicle platform remarkably well. Hence, not only the specific active suspension system can increase the vehicle mobility and maneuverability, provide a stable platform for weapon firings and improved target hit probabilities, but it can also lower the power consumption of the vehicle, reduce the absorbed power by the driver, and improve the overall fuel economy of the vehicle.

INTRODUCTION

Modern military vehicles require high performance in their mobility, maneuverability, and stability, particularly in harsh terrains and/or off-road environment. In such circumstances, a vehicle must be able to provide a good, or at least acceptable, ride quality and handling regardless of the presence of shock loads and random terrain disturbances. In addition, it must be able to keep its body and/or its gun-turret steady in order to provide a stable platform for weapon firings and improved target hit probabilities. It is well-known that any vehicle equipped with an active suspension system can provide and, in certain circumstances, fulfill such requirements. However, most active suspension systems are known to require substantial amount of energy to produce the control forces, for instance, in racing cars where up to 40% of the engine power may be consumed by the active suspension mechanism [1].

Recent research in the area of active suspension platforms has focused on low power consumption required to stabilize a vehicle. A novel active suspension system that offers such low power consumption originated in [2] has been carefully studied in [2-7], and some of its aspects in [8-10]. The vital component of this particular system is a mass moving on a rail under the influence of a compressed spring, thereby transforming a positive stiffness spring into a negative stiffness spring. This mechanism is placed on a carrier which is connected to a set of ordinary springs and dampers to form an active suspension structure (see details in the next section). It was shown in [2,3] that the system resulted in low power consumption by the vehicle actuators over the relevant range of its displacements. In references [4,5,7], the unforced dynamics or open-loop system and stability of the equilibrium points have been analyzed thoroughly. They showed that the system behaved similar to that of the Duffing oscillator [7,11,12]. The comprehensive analyses and extensive simulations demonstrated that the system can have up to three equilibrium points depending on the system parameters; in particular, in [7], Dumont *et al.* extended the

analysis of the unforced, i.e., no control, system by taking into account the friction between the moving mass and the rail. It was shown that, with friction, there exist three separate stick zones centered on the critical points such that the moving mass may remain at rest or stuck if it is in any one of these zones. However, in contrast to the open-loop stability studies, not much has been done in the area of closed-loop control, except in [2]. In [2], the linear quadratic regulator (LQR) control scheme using a linearized model obtained by a first-order Taylor series approximation was investigated. The closed-loop performance resulting from the Taylor series linearization approach may not be the best that could be achieved. Inspired by the works of [4,5,7], and in view of the fact that the active suspension system incorporating a negative stiffness spring considered here is a minimum-phase nonlinear system which is well suited for nonlinear control designs, we will employ the feedback linearization methodologies and techniques [13-16] for the analysis and design of nonlinear controls for this particular system. Furthermore, a Luenberger observer [17] for the system is constructed for the synthesis and leads to the design of an observer-based nonlinear control system.

The paper is organized as follows. The mathematical modeling and nonlinear control problem formulation for the negative stiffness element as well as the active suspension system are described in the next section, followed by the designs of the tracking nonlinear controls and observer. Next, extensive simulations demonstrate the effectiveness of the proposed observer-based nonlinear closed-loop control system, including the results of power consumptions and the absorbed power by drivers. Finally, some concluding remarks are presented in the last section.

THE MODEL

In this section, we introduce the mathematical model of the negative stiffness spring element, and incorporate it into the overall active suspension system. We know that the force associated with a conventional spring of nominal length L_o, and spring constant k_o with displacement $p(t)$ is given by $F(t) = k_o p(t)$. For the negative stiffness spring element, the conventional spring is compressed to the length of L, one end is fixed and the other end is attached to a small movable mass as shown in figure 1(a).

In this setup, the mass can move away from its equilibrium at the center in both directions as the compressed spring always tries to extract itself to its nominal length. The associated horizontal force $F_T(t)$ when the mass moves to the right as in figure 1(b) is given by [2-7]

$$F_T = -kx\left(1 - \frac{L_o}{\sqrt{x^2 + L^2}}\right), \qquad (1)$$

where $x = x(t)$ is the distance of the mass away from the center, and k the normalized spring stiffness given by k_o / m [7]. The force F_T in (1) behaves as a force generated by the spring with a stiffness coefficient that is negative [4,7]. It is remarked here that the operating range in this setup is confined to $|x| < \sqrt{L_o^2 + L^2}$. Defining $\Psi(x) \triangleq F_T$, we obtain the nonlinear force function as a function of the displacement x that represents the negative stiffness spring element. Details of the stability analysis of equation (1) can be found in [2,4,5,7].

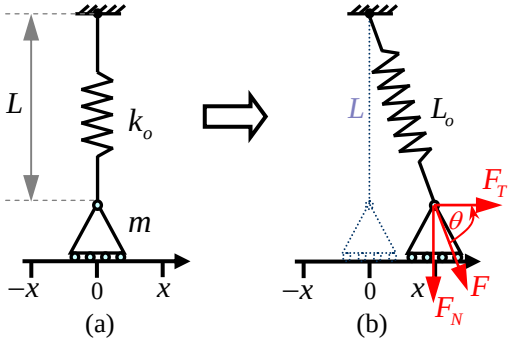

Figure 1: Negative stiffness spring element diagram.

This negative stiffness spring element is incorporated into the active suspension system by turning the diagram in figure 1 clockwise by 90 degrees so that the force F_T is in the vertical direction. A mass-spring-damper diagram of the resulting quarter-vehicle active suspension system is depicted in figure 2.

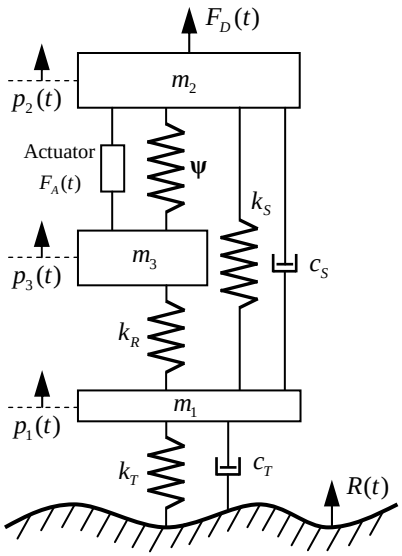

Figure 2: Active suspension incorporating a nonlinear negative stiffness spring.

Let $p_1(t)$, $p_2(t)$ and $p_3(t)$ be the displacement of each mass; the unsprung mass m_1 represents the mass of the wheel/tire and the suspension structure, the sprung mass m_2 acts as the body of a quarter vehicle, and the unsprung mass m_3 forms an active control mechanism. The constant parameters *k* and *c* characterize the stiffness and damping coefficients of the springs and dampers, respectively; the subscript *T* denotes wheel/tire, *S* and *R* denote suspension and the control mechanism, accordingly. The negative stiffness spring is represented by $\Psi = \Psi(p_3 - p_2)$. The actuator $F_A(t)$ provides the reaction force required to overcome the deflection of the vehicle platform; $F_D(t)$ represents the force resulted from the driver acting on the suspension system; and $R = R(t)$ represents the road profile. A more detailed description of the overall system can be found in [2-5].

With the definitions above, it can easily be shown that the model of the system is given by

$$\left.\begin{aligned} m_1\ddot{p}_1 = k_T(R - p_1) + c_T(\dot{R} - \dot{p}_1) + k_S(p_2 - p_1) + \\ c_S(\dot{p}_2 - \dot{p}_1) + k_R(p_3 - p_1) - m_1 g, \end{aligned}\right\} \quad (2)$$

$$\left.\begin{aligned} m_2\ddot{p}_2 = k_S(p_1 - p_2) + c_S(\dot{p}_1 - \dot{p}_2) - \Psi(p_3 - p_2) + \\ F_D + F_A - m_2 g, \end{aligned}\right\} \quad (3)$$

$$m_3\ddot{p}_3 = k_R(p_1 - p_3) + \Psi(p_3 - p_2) - F_A - m_3 g\,. \quad (4)$$

The nonlinear spring function $\Psi(p_3 - p_2)$ in equations (3)-(4) is given by, from equation (1),

$$\Psi(p_3 - p_2) = -k(p_3 - p_2)\left(1 - \frac{L_o}{\sqrt{(p_3 - p_2)^2 + L^2}}\right), \quad (5)$$

where L_o is the nominal length of the spring, *L* the compressed length of the spring, and *k* the normalized spring stiffness.

The stability of the equilibrium points of the system given by equations (2)-(4) has been investigated thoroughly in [4,5,7]. The system has three possible steady states depending on the system parameters, including the parameters of the negative stiffness spring structure. It was shown that in the case of one steady state, the single equilibrium point is stable. However, the characteristic of the overall system was similar to the case of using an ordinary spring, thus diminishing the importance and all the contributions of a negative stiffness spring. In the case of two steady states, the system was structurally unstable and therefore impractical. In the last case of three steady states, the equilibrium nearest the origin was found to be unstable while the others two were stable. The results in [4] concluded that the three-steady state case was suitable for active suspension control design that could result in low power consumption.

To formulate the model given by equations (2)-(4) for a control analysis and synthesis, we define the state variables as $\left[x_1\ x_2\ x_3\ x_4\ x_5\ x_6\right]^T = \left[p_1\ \dot{p}_1\ p_2\ \dot{p}_2\ p_3\ \dot{p}_3\right]^T$; the control input $u(t) = F_A(t)$; and the measured output $y(t) = x_3(t)$. A nonlinear state-space model can then be written in the following general form:

$$\dot{\mathbf{x}} = \mathbf{f}(\mathbf{x}) + \mathbf{g}(\mathbf{x})u\,, \quad (6)$$

$$y = h(\mathbf{x}) = x_3\,, \quad (7)$$

where **f(x)** and **g(x)** are given by, respectively,

$$\mathbf{f}(\mathbf{x}) = \begin{bmatrix} x_2 \\ \left(-\frac{k_T}{m_1}x_1 - \frac{c_T}{m_1}x_2 + \frac{k_S}{m_1}(x_3 - x_1) + \frac{c_S}{m_1}(x_4 - x_2) + \frac{k_R}{m_1}(x_5 - x_1) - \right. \\ \left. g + \frac{k_T}{m_1}R + \frac{c_T}{m_1}\dot{R}\right) \\ x_4 \\ \frac{k_S}{m_2}(x_1 - x_3) + \frac{c_S}{m_2}(x_2 - x_4) - \frac{1}{m_2}\Psi(x_5 - x_3) - g + \frac{1}{m_2}F_D \\ x_6 \\ \frac{k_R}{m_3}(x_1 - x_5) + \frac{1}{m_3}\Psi(x_5 - x_3) - g \end{bmatrix}, \quad (8)$$

and

$$\mathbf{g}(\mathbf{x}) = \begin{bmatrix} 0 & 0 & 0 & \frac{1}{m_2} & 0 & -\frac{1}{m_3} \end{bmatrix}^T. \quad (9)$$

Examination of equations (6)-(9) reveals that the nonlinear term $\Psi(x_5 - x_3)$ and the gravitational constant g can be cancelled by feedback linearization through both of the input-state channels. In addition, the terms consisting of the road profile *R(t)*, its time derivative $\dot{R}(t)$, and the force resulting from the driver $F_D(t)$ in equation (8) can be considered as disturbance inputs. In this study, we assume that all disturbances are measurable and/or computable. It

will be shown in the next section through the design of the nonlinear controller that the driver disturbance $F_D(t)$ can be handled by a feed-forward/feedback control law, and the road disturbance $R(t)$ and $\dot{R}(t)$, by themselves, are completely decoupled from the output of interested and therefore will not affect the output.

NONLINEAR CONTROL DESIGN

The nonlinear control design based on the input-output feedback linearization technique [13-16] can be applied to overcome the nonlinearity of the active suspension system described in equations (6)-(9).

Consider a general single-input single-output (SISO) nonlinear system described by

$$\dot{\mathbf{x}} = \mathbf{f}(\mathbf{x}) + \mathbf{g}(\mathbf{x})u\,, \quad \mathbf{f},\mathbf{g}: D \subset \mathbb{R}^n \to \mathbb{R}^n\,, \tag{10}$$

$$y = h(\mathbf{x})\,, \qquad h: D \subset \mathbb{R}^n \to \mathbb{R}\,, \tag{11}$$

where $\mathbf{f},\mathbf{g}: D \subset \mathbb{R}^n \to \mathbb{R}^n$ are smooth vector fields, $h: D \subset \mathbb{R}^n \to \mathbb{R}$ a smooth function (output measurement), and D is an open set. Briefly, the input-output feedback linearization methodology is to find a transformation function $\mathbf{z} = \mathbf{T}(\mathbf{x})$ that transforms the original nonlinear system in the *x*-coordinates to a linear system in the *z*-coordinates by differentiating the output function ρ times with respect to *t*, i.e., $y^{(\rho)}(t)$, until the input $u(t)$ appears. The differentiation process is then terminated and ρ is called the *relative degree* of the system.

In the present case, $\mathbf{f}(\mathbf{x})$ and $\mathbf{g}(\mathbf{x})$ are as given in equations (8) and (9), respectively, while $y = h(\mathbf{x}) = x_3$. We proceed by differentiating the output $y(t) = x_3(t)$ twice to obtain

$$\left.\begin{aligned} \dot{y} &= x_4, \\ \ddot{y} &= \frac{k_S}{m_2}(x_1 - x_3) + \frac{c_S}{m_2}(x_2 - x_4) - \frac{1}{m_2}\Psi(x_5 - x_3) - \\ &\qquad g + \frac{1}{m_2}F_D + \frac{1}{m_2}u, \end{aligned}\right\} \tag{12}$$

where the input $u(t)$ appears in the second equation in equation (12), implying that the relative degree is two, i.e., $\rho = 2$. Also, the driver disturbance $F_D(t)$ shows up in the same equation, thus it can be cancelled by the feed-forward control signal as it is measurable [18,19]. It is worth noting here that the road disturbance $R(t)$ and its derivative $\dot{R}(t)$ do not appear in equation (12) which implies that the output function $y(t) = x_3(t)$ is totally decoupled from the road disturbances [16,18].

The fact that the relative degree is $\rho = 2$ implies that the original nonlinear system can only be partially linearized. It is not difficult to show that the transformation or diffeomorphism $\mathbf{z} = \mathbf{T}(\mathbf{x})$ associated with equations (6)-(9) is given by

$$\mathbf{z} = \mathbf{T}(\mathbf{x}) \triangleq \begin{bmatrix} \boldsymbol{\xi} \\ \hline \boldsymbol{\eta} \end{bmatrix} = \left[\begin{array}{c} x_3 \\ x_4 \\ \hline x_1 \\ x_2 \\ x_5 \\ m_2 x_4 + m_3 x_6 \end{array}\right], \tag{13}$$

where $\boldsymbol{\xi}(t)$ and $\boldsymbol{\eta}(t)$ represent, respectively, the *external* dynamic states which are controllable and observable, and the *internal* dynamic states which are not.

Equation (13) yields

$$\begin{bmatrix} \dot{\boldsymbol{\xi}} \\ \dot{\boldsymbol{\eta}} \end{bmatrix} = \frac{\partial \mathbf{T}(\mathbf{x})}{\partial \mathbf{x}}\dot{\mathbf{x}} = \frac{\partial \mathbf{T}(\mathbf{x})}{\partial \mathbf{x}}\left[\mathbf{f}(\mathbf{x}) + \mathbf{g}(\mathbf{x})u\right]. \tag{14}$$

From equations (6) and (14), we obtain the *normal form*

$$\dot{\boldsymbol{\xi}} = \mathbf{A}_{\xi}\boldsymbol{\xi} + \mathbf{B}_{\xi}v\,, \tag{15}$$

$$\dot{\boldsymbol{\eta}} = \mathbf{f}_{\mathbf{o}}(\boldsymbol{\xi}, \boldsymbol{\eta})\,, \tag{16}$$

$$y = \mathbf{C}_{\xi}\boldsymbol{\xi}\,, \tag{17}$$

where $v(t)$ is called the transformed input, $\mathbf{A}_{\xi} = \begin{bmatrix} 0 & 1 \\ 0 & 0 \end{bmatrix}$, $\mathbf{B}_{\xi} = \begin{bmatrix} 0 \\ 1 \end{bmatrix}$, $\mathbf{C}_{\xi} = \begin{bmatrix} 1 & 0 \end{bmatrix}$, and

$$\mathbf{f}_{\mathbf{o}}(\boldsymbol{\xi}, \boldsymbol{\eta}) = \begin{bmatrix} \eta_2 \\ \frac{1}{m_1}\left(\begin{array}{c}(-k_T - k_S - k_R)\eta_1 - (c_T + c_S)\eta_2 + k_R\eta_3 \\ + k_S\xi_1 + c_S\xi_2 - m_1 g + k_T R + c_T\dot{R}\end{array}\right) \\ \frac{1}{m_3}(\eta_4 - m_2\xi_2) \\ \left(\begin{array}{c}(k_S + k_R)\eta_1 + c_S\eta_2 - k_R\eta_3 - k_S\xi_1 - c_S\xi_2 \\ -(m_2 + m_3)g + F_D\end{array}\right) \end{bmatrix}. \tag{18}$$

Note that $\mathbf{A}_\xi$, $\mathbf{B}_\xi$, and $\mathbf{C}_\xi$ are in controllable canonical form and the Jacobian matrix in equation (14) has the form

$$\frac{\partial \mathbf{T}(\mathbf{x})}{\partial \mathbf{x}} = \begin{bmatrix} 0 & 0 & 1 & 0 & 0 & 0 \\ 0 & 0 & 0 & 1 & 0 & 0 \\ 1 & 0 & 0 & 0 & 0 & 0 \\ 0 & 1 & 0 & 0 & 0 & 0 \\ 0 & 0 & 0 & 0 & 1 & 0 \\ 0 & 0 & 0 & m_2 & 0 & m_3 \end{bmatrix}, \tag{19}$$

which is nonsingular for all $\mathbf{x} \in \mathbb{R}^6$. Therefore **T(x)** is a global diffeomorphism for the system described by equation (6).

The *external dynamics* of the subsystem described by equation (15) can be controlled by the transformed input $v(t)$ using any well-known linear control design, such as pole placement, proportional-integral-derivative (PID) control, and linear quadratic regulator (LQR). The *internal dynamics* of the subsystem described by equation (16) cannot be controlled, and also do not affect the output responses irrespective whether $\boldsymbol{\eta}(t)$ is stable or unstable. However, for a partially linearizable system, the stability of equation (16) is crucial in designing feedback controllers for the overall system. It follows that the stability of the internal dynamics can be analyzed by the *zero dynamics* obtained by setting $\boldsymbol{\xi} = \mathbf{0}$ in equation (16)

$$\dot{\boldsymbol{\eta}} = \mathbf{f}_o(\mathbf{0}, \boldsymbol{\eta}). \tag{20}$$

Furthermore, since all the disturbances in equation (20) act as inputs to the zero dynamics and are not a function of $\boldsymbol{\eta}(t)$, the stability of the zero dynamics can be analyzed by the unforced equation,

$$\dot{\boldsymbol{\eta}} = \mathbf{A}_{\boldsymbol{\eta}} \boldsymbol{\eta}, \tag{21}$$

where

$$\mathbf{A}_{\boldsymbol{\eta}} = \begin{bmatrix} 0 & 1 & 0 & 0 \\ -\frac{1}{m_1}(k_T + k_S + k_R) & -\frac{1}{m_1}(c_T + c_S) & \frac{k_R}{m_1} & 0 \\ 0 & 0 & 0 & \frac{1}{m_3} \\ k_S + k_R & c_S & -k_R & 0 \end{bmatrix}. \tag{22}$$

Using the numerical values provided in the next section, all the eigenvalues of $\mathbf{A}_{\boldsymbol{\eta}}$ are located on the left-half complex plane. We conclude that the zero dynamics are stable and the system in equation (6) is *minimum phase*. Therefore, the overall system can be partially linearized by the linearizing control law

$$\left.\begin{aligned} u = m_2 v - k_S x_1 - c_S x_2 + k_S x_3 + c_S x_4 + \\ \Psi(x_5 - x_3) + m_2 g - F_D. \end{aligned}\right\} \tag{23}$$

Asymptotic Output Tracking

Let the control objective be steering the position $y(t) = x_3(t)$ of the vehicle body or mass m_2 to a desirable position (reference output) y_r, i.e., $x_3(t) \to y_r$ as $t \to \infty$; this gives rise to a tracking control problem. A suitable control law for the transformed input $v(t)$ in equations (15) and (23) is given by

$$v = -\mathbf{K}_\xi \boldsymbol{\xi} + K_r y_r = -K_1 x_3 - K_2 x_4 + K_r y_r, \tag{24}$$

where the constant feedback gain matrix $\mathbf{K}_\xi = \begin{bmatrix} K_1 & K_2 \end{bmatrix}$ is determined such that $\mathbf{A}_{cl} \triangleq \mathbf{A}_\xi - \mathbf{B}_\xi \mathbf{K}_\xi$ is Hurwitz, that is, all eigenvalues of $\mathbf{A}_{\xi cl}$ lie in the open left-half complex plane. Numerous design methods from the powerful linear control theory can be used to determine the gain $\mathbf{K}_\xi$, such as the pole placement, PID, and LQR techniques; while the gain K_r in equation (24) is a scalar constant tracking gain determined by

$$K_r = \left(\mathbf{C}_\xi \left(-\mathbf{A}_{cl}\right)^{-1} \mathbf{B}_\xi\right)^{-1}. \tag{25}$$

OBSERVER DESIGN

It is seen from the transformed control law of equation (24) and the linearizing control law of equation (23) that online knowledge of all states is required to compute both control laws. In this section, we present the estimation of the external dynamic states, that is, $x_3(t)$ and $x_4(t)$. However, the estimation of the internal dynamic states $x_1(t)$, $x_2(t)$, $x_5(t)$ and $x_6(t)$ is not possible and thus we assume that all knowledge of the internal dynamic states is available.

Consider again the external dynamics of equation (15) and the output equation (17). Since the pair $\left[\mathbf{A}_\xi, \mathbf{C}_\xi\right]$ is observable, that is, $rank\left[\mathbf{C}_\xi^T \quad \mathbf{A}_\xi^T \mathbf{C}_\xi^T\right] = 2$, it follows that a Luenberger observer [17] for equation (15) can be constructed as

$$\dot{\hat{\boldsymbol{\xi}}} = \mathbf{A}_{\xi cl} \hat{\boldsymbol{\xi}} + \mathbf{B}_\xi v + \mathbf{L}_\xi y, \tag{26}$$

where $\mathbf{A}_{\xi cl} \triangleq \mathbf{A}_{\xi} - \mathbf{L}_{\xi}\mathbf{C}_{\xi}$ is the observer matrix, and the gain matrix $\mathbf{L}_{\xi} \in \mathbb{R}^{2\times 1}$ is determined such that $\mathbf{A}_{\xi cl}$ is Hurwitz. Defining the estimation error as $\tilde{\boldsymbol{\xi}} = \boldsymbol{\xi} - \hat{\boldsymbol{\xi}}$, it can be shown through an error analysis that

$$\dot{\tilde{\boldsymbol{\xi}}} = \mathbf{A}_{\xi cl}\tilde{\boldsymbol{\xi}}. \tag{27}$$

Since $\mathbf{A}_{\xi cl}$ is Hurwitz, it follows that the estimation error $\tilde{\boldsymbol{\xi}}(t) \to 0 \;\Rightarrow\; \hat{\boldsymbol{\xi}}(t) \to \boldsymbol{\xi}(t)$ as $t \to \infty$. Using the estimated states obtained from equation (26), the observer-based control laws of equation (24) and (23) can be implemented as

$$\hat{v} = -K_1\hat{x}_3 - K_2\hat{x}_4 + K_r y_r, \tag{28}$$

$$u = \left.\begin{array}{r} m_2\hat{v} - k_S x_1 - c_S x_2 + k_S\hat{x}_3 + c_S\hat{x}_4 + \\ \Psi\left(x_5 - \hat{x}_3\right) + m_2 g - F_D. \end{array}\right\} \tag{29}$$

Finally, substituting equation (29) into equation (6), we obtain the overall closed-loop nonlinear active suspension system with a negative stiffness spring in the *x*-coordinates as:

$$\dot{\mathbf{x}} = \mathbf{f}(\mathbf{x}) + \mathbf{g}(\mathbf{x})\begin{bmatrix} m_2\hat{v} - k_S x_1 - c_S x_2 + k_S\hat{x}_3 + c_S\hat{x}_4 + \\ \Psi\left(x_5 - \hat{x}_3\right) + m_2 g - F_D. \end{bmatrix}, \tag{30}$$

where $\hat{v}(t)$ is given by equation (28). The next task is to conduct an extensive simulation studies; the main results are reported below.

SIMULATION RESULTS

MATLAB simulations were conducted to demonstrate the performances of the proposed observer-based controller and the overall closed-loop nonlinear control system given by equation (30). The system parameters were chosen for the three-equilibrium points case are shown in table 1.

Table 1: System parameter values

Symbol	Description	Value
m_1	Wheel/tire mass	50 kg
m_2	Quarter vehicle mass	400 kg
m_3	Active control mechanism mass	5 kg
k_T	Wheel/tire stiffness coefficient	18,000 kg/s^2
k_S	Suspension spring stiffness coefficient	3,000 kg/s^2
k_R	Control mechanism spring stiffness coefficient	40,000 kg/s^2
c_T	Wheel/tire damping coefficient	100 kg/s
c_S	Suspension damping coefficient	100 kg/s
g	Gravity	9.8 m/s^2
k	Normalized negative stiffness spring coefficient	30,000 kg/s^2
L	Compressed length of the negative stiffness spring	0.5 m
L_0	Nominal length of the negative stiffness spring	1 m

The control gain matrix $\mathbf{K}_{\xi} = \begin{bmatrix} 17.5 & 6.75 \end{bmatrix}$ for the transformed control law of equation (24) was computed by placing the control poles at $-3.5 \pm j3.57$ of the complex plane, which corresponds to a closed-loop damping ratio of $\zeta = 0.7$ and a natural frequency of $\omega_n = 5$ rad/s. The tracking gain in equation (25) was found to be $K_r = 25$. Similar to the control design, the observer gain matrix $\mathbf{L}_{\xi} = \begin{bmatrix} 6 & 5 \end{bmatrix}^T$ was obtained by placing the observer poles at -1 and -5 of the complex plane.

Two cases of simulations were conducted: regulation and tracking. In the regulation case, the initial condition was $\mathbf{x}_0 = \{$-0.24, 0, -0.1, 0, -0.35, 0$\}$ which is close to the equilibrium point of the unforced system. A step input for the driver disturbance was chosen as $F_D = 75g$, and a sinusoidal road profile $R(t) = 0.05\sin(8t)$ were activated at time $t = 5$ s, and $t = 10$ s, respectively. Figures 3-8 show the responses of $x_1(t) - x_6(t)$. It is observed that the displacement $x_3(t)$ of the vehicle body in figure 5 quickly converged to zero while the movement of the wheel in figure 3 and the suspension in figure 7 converged to their steady states at slower rates. It is also seen clearly that the displacement of the wheel/tire, and the suspension reacted to the disturbances at the time $t = 5$ s, and $t = 10$ s but the control actuator force in figure 9 kept the vehicle body displacement unaffected from both disturbances which showed that the ride was smooth. Furthermore, the results in figure 5 and 6 show excellent convergences of the estimates $\hat{x}_3(t)$ and $\hat{x}_4(t)$ to the external dynamic states $x_3(t)$ and $x_4(t)$, respectively.

Figure 10 provides a comparison of the control input $u(t)$ between using negative stiffness spring and ordinary spring. It is shown that the system incorporating the negative stiffness element requires much less actuator force to stabilize the vehicle than the system with ordinary spring.

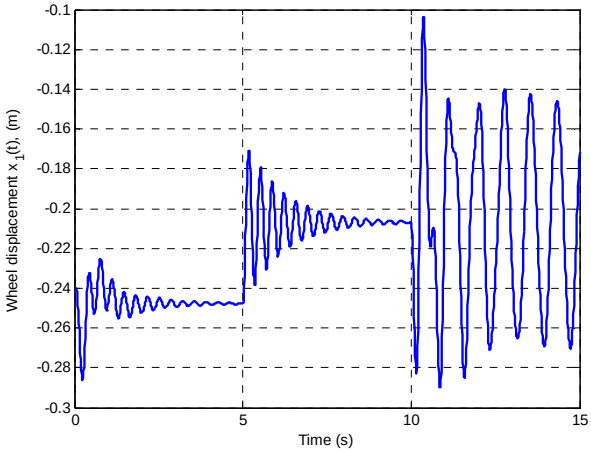

Figure 3: Wheel displacement, regulator case.

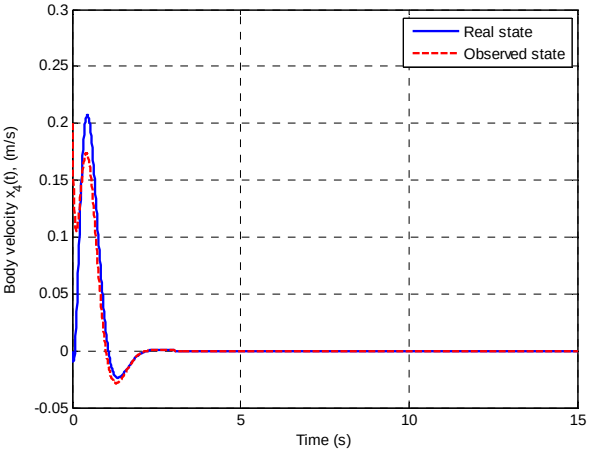

Figure 6: Vehicle body velocity, regulator case.

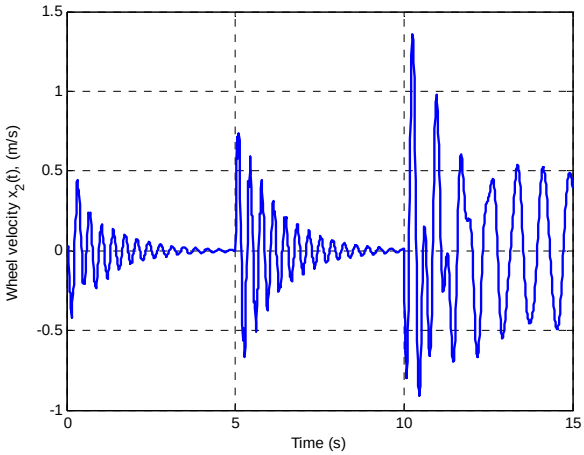

Figure 4: Wheel velocity, regulator case.

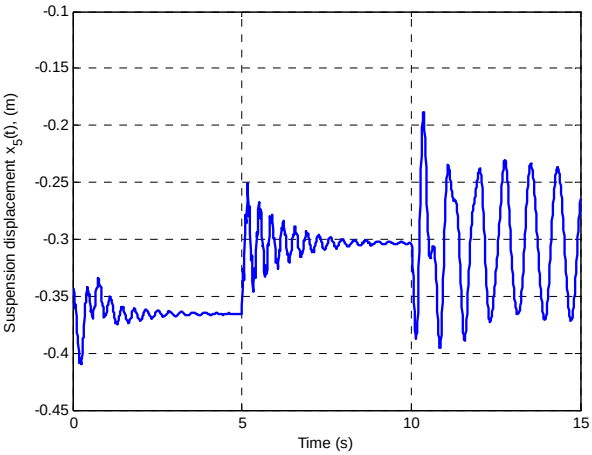

Figure 7: Suspension displacement, regulator case.

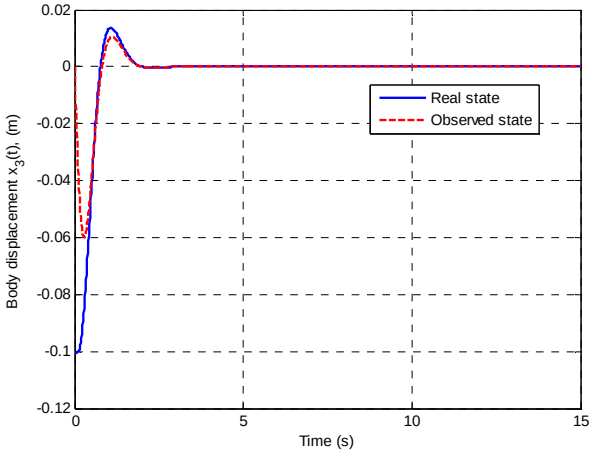

Figure 5: Vehicle body displacement, regulator case.

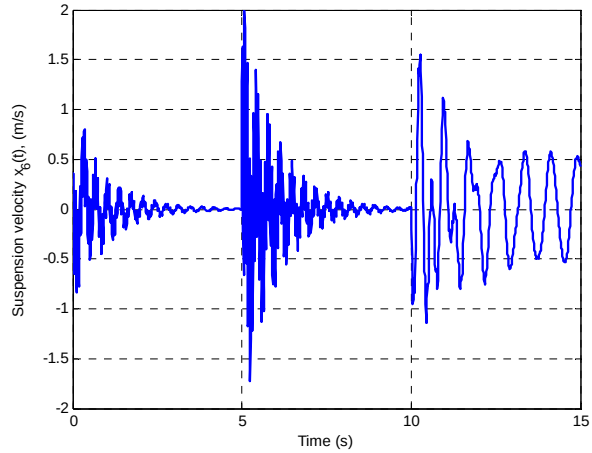

Figure 8: Suspension velocity, regulator case.

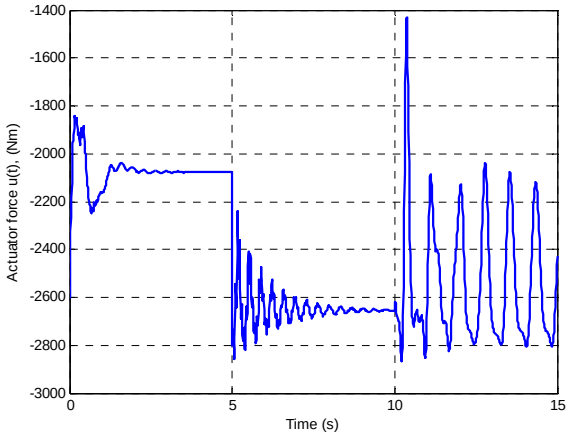

Figure 9: Actuator control $u(t)$, regulator case.

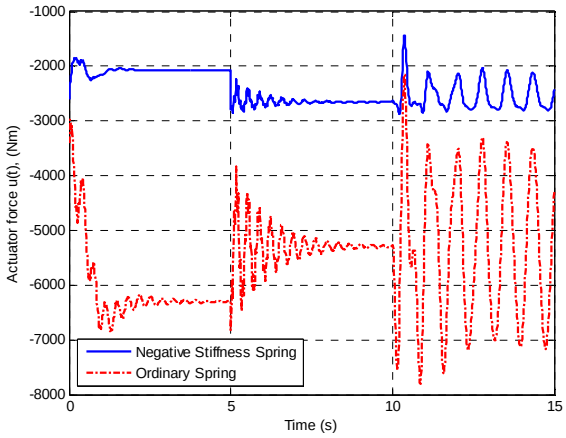

Figure 10: Comparison of the control $u(t)$, regulator case.

For the tracking case, the simulation results are shown in figures 11–18 in the same manner as the regulator case. The output reference in this case was set to $y_r = 0.1$ and the initial condition was $\mathbf{x}_0 = \mathbf{0}$. Both disturbances were applied at the same time as before at 5 and 10 seconds but the driver disturbance was a sinusoidal signal $F_D(t) = 75g\sin(2t)$ with a low frequency [6].

Figure 13 shows that vehicle body quickly settled to the reference value $y_r = 0.1$, and no interference from the disturbances. Figure 13 and 14 also show good convergences of the observer states $\hat{x}_3(t)$ and $\hat{x}_4(t)$. The actuator control input $u(t)$ and a comparison of the control $u(t)$ used in the active suspension system with/without the negative stiffness spring are shown in figure 17 and 18, respectively. Again, it shows that the system with the negative stiffness spring needed much less actuator force to stabilize the vehicle body which implies much less energy consumption.

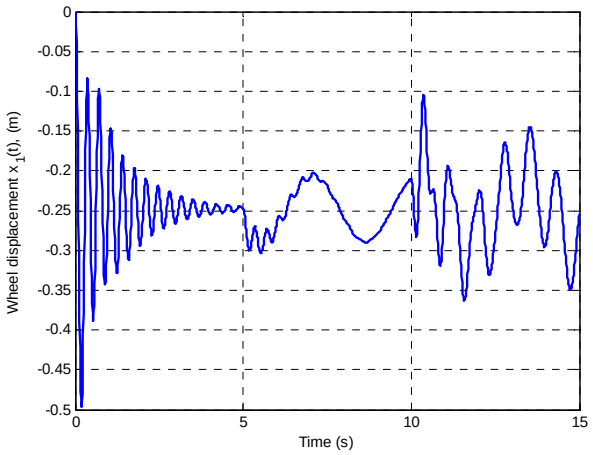

Figure 11: Wheel displacement, tracking case.

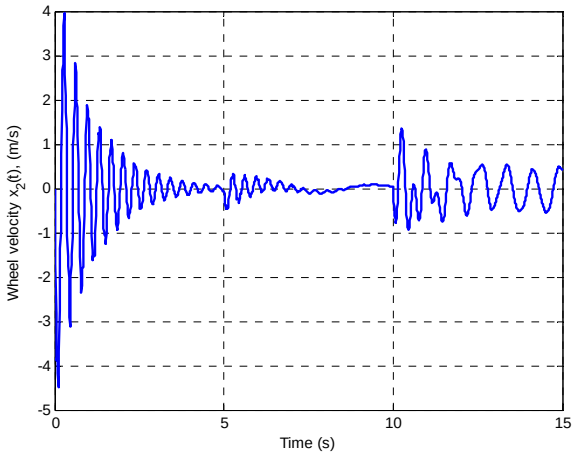

Figure 12: Wheel velocity, tracking case.

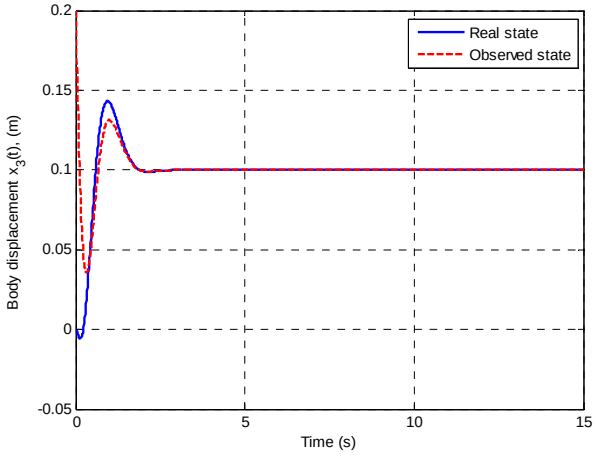

Figure 13: Vehicle body displacement, tracking case.

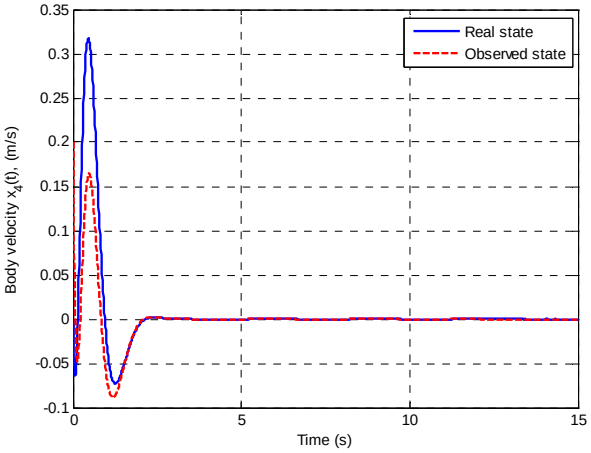

Figure 14: Vehicle body velocity, tracking case.

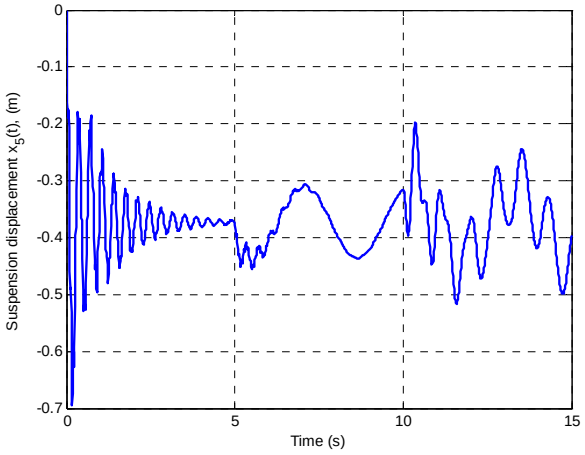

Figure 15: Suspension displacement, tracking case.

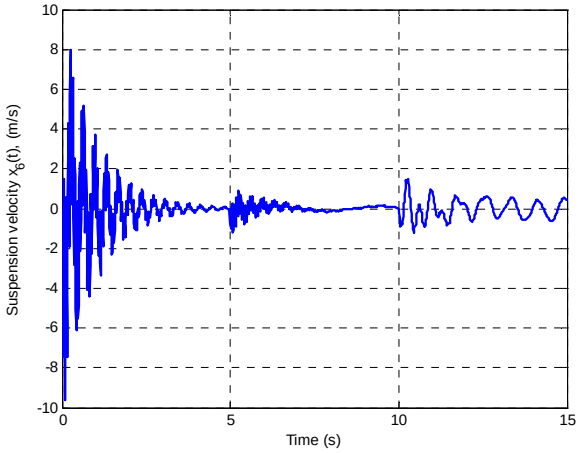

Figure 16: Suspension velocity, tracking case.

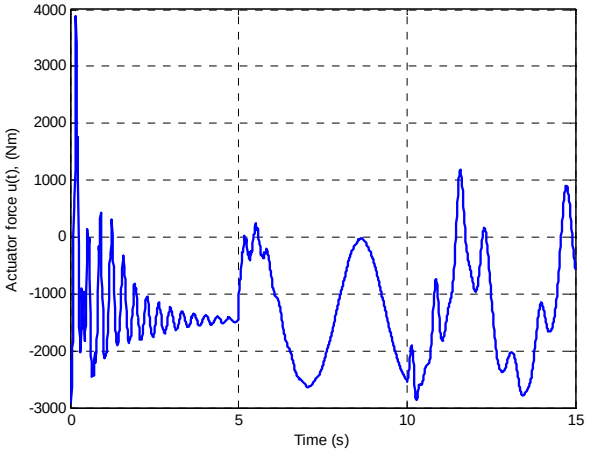

Figure 17: Actuator control $u(t)$, tracking case

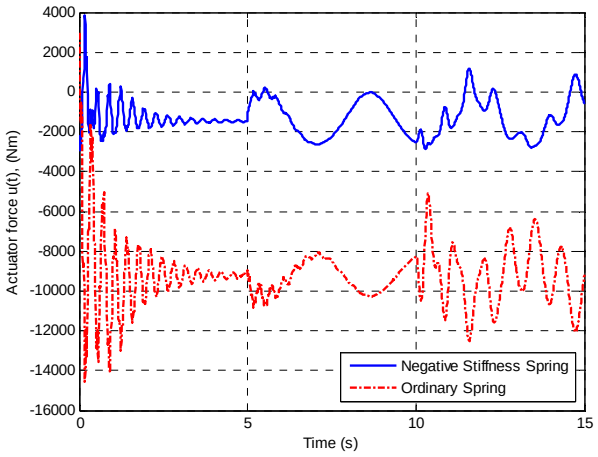

Figure 18: Comparison of the control $u(t)$, tracking case

Two cases of the simulation results presented show that the observer-based nonlinear controller can provide impressive performance in terms of stabilizing the vehicle body, rejecting all harsh disturbances, and ultimately resulting in significant improved driver's ride comfort. In military vehicle applications, ride comfort is not an issue of luxury but safety. Drivers could be injured by exposing them to severe vibrations for an extended period of time. There are many criteria to quantify ride comfort or to assess human sensitivity to vibrations. Two criteria are presented here: the absorbed power of less than 6 W [20] and the vibration dose of less than 15 m^4/s^7 [21]. Table 2 displays the computation results of such measures for both cases: regulator and tracking. Both criteria are well below the maximum values allowed.

Table 2: Power consumption and absorbed power.

Simulation case	Absorbed power (W)	Vibration dose (m^4/s^7)
Regulator	3.35×10^{-4}	6.02×10^{-11}
Tracking	1.2×10^{-3}	8.63×10^{-10}

CONCLUSION

The analysis and design of an observer-based nonlinear controller using the feedback linearization technique have been considered for an active suspension system incorporating a negative stiffness spring. The advantage of this system is that it consumes less energy for operation, thereby making it attractive not only to vehicle suspension applications but also to other platform stabilization problems. In this paper, we show that the two disturbances of the system: driver load and road profile can be completely decoupled from the output; in other words, the vehicle body displacement will not be affected by these disturbances. This directly translates into a greatly enhanced performance in ride comfort. The simulation results also show that the controller performs extremely well in the tracking task, regardless of the initial conditions. In addition, the computed results of the absorbed power and vibration dose show interesting and promising results. The technique and methodology developed in this paper are readily applicable to the automotive and defense industries, especially military vehicle systems. The design of a prototype system is under consideration.

REFERENCES

[1] J. Dominy and D. N. Bulman, "An active suspension for a Formular One Grand Prix racing car", Transactions of the ASME Journal Dynamic Systems, Measurements and Control, vol 107, pages 73-78, 1995.

[2] D. S. Cameron, "Platform Stabilization with a Novel Active Suspension", Ph.D. dissertation, Oakland University, MI, U.S.A., 1999.

[3] D. S. Cameron, N. A. Kheir and M. Shillor, "Low energy active platform stabilizing suspension system", Proceedings of the world Automation Congress ISIAC, Hawaii, U.S.A., 2000.

[4] W. A. Lindsey, A. M. Spagnuolo, J. C. Chipman and M. Shillor, "Numerical Simulations of Vehicle Platform Stabilization", Mathematical and Computer Modelling, vol 41, pages 1389-1402, 2005.

[5] D. S. Cameron, J. C. Chipman, N. Kheir and M. Shillor, "Model and Numerical Simulations of Vehicle Platform Stabilization", 2001.

[6] D. S. Cameron and N. A. Kheir, "On the Modeling of Ground Vechicle Attitude Control", Proceedings of the 35th conference on Decision and Control, Kobe, Japan, December, pages 3570-3574, 1996.

[7] Y. Dumont, D. Goeleven, M. Rochdi and M. Shillor, "Frictional Contact of a Nonlinear Spring", Mathematical and Computer Modelling, vol 31, pages 83-97, 2000.

[8] D. Hrovat, D. L. Margolis and M. Hubbard, "An approach toward the optimal semi-active suspension", Transactions of the ASME Journal Dynamic Systems, Meas. and Control, vol 110, pages 288-296, 1988.

[9] J. Darling, R. E. Dorey and T. J. Ross-Martin, "A low cost active anti-roll suspension for passenger cars", Transactions of the ASME Journal Dynamic Systems, Meas. and Control, vol 114 (3), pages 599-605, 1992.

[10] P. J. Th. Venhovens, A. C. M. Van der Knapp and H. B. Pacejka, "Semi-active attitude and vibration control", International Journal of Vehicle Mech. Mob., Vehicle System Dyn., vol 22, pages 359-381, 1993.

[11] J. Argyris, G. Faust and M. Haase, “An Exploration of Chaos”, Elsevier Science, Amsterdam, 1994.

[12] S. Wiggins, “Introduction to applied dynamical systems and chaos”, Springer, New York, 1990.

[13] H. K. Khalil, “Nonlinear Systems”, 3rd edition, Prentice Hall, New Jersey, 2002.

[14] H. J. Marquez, “Nonlinear Control Systems: Analysis and Design”, John Wiley & Sons, New Jersey, 2003.

[15] A. Isidori, ”Nonlinear Control Systems”, 3rd edition, Springer-Verlag, New York, 1995.

[16] M. A. Henson and D. E. Seborg, “Nonlinear Process Control”, Prentice Hall, New Jersey, 1997.

[17] D. G. Luenberger, “Observing the state of a linear system”, IEEE Transactions on Military Electronics, pages 74-80, April 1964.

[18] P. Daoutidis and C. Kravaris, "Synthesis of Feedforward/State Feedback Controller for Nonlinear Processes", AIChE Journal, vol 35, number 10, pages 1602-1616, 1989.

[19] C. I. Byrnes and A. Isidori, "Nonlinear Disturbance Decoupling with Stability", In Proceedings of IEEE Conference on Decision and Control, Los Angeles, vol 26, pages 513-515, 1987.

[20] R. A. Lee and W. F. Lins, “Human Vibration Measuring Instrument”, AD-785648, Army Tank-Automotive Command, Warren, Michigan, 1973.

[21] E. Guglielmino *et al.*, “Semi-active Suspension Control”, Springer-Verlag, London, 2008.